J. Mol. Biol. (1996) **264**, 757–769

JMB

Solution Structure of a Parallel Left-handed Double-helical Gramicidin-A Determined by 2D ^{1}H NMR

Y. Chen[1], A. Tucker[2] and B. A. Wallace[1]*

[1]*Department of Crystallography, Birkbeck College, University of London, London WC1E 7HX, UK*

[2]*Biomedical NMR Centre Department of Chemistry Birkbeck College, University of London, London WC1E 7HX, UK*

*Corresponding author

The structure of a parallel left-handed double-helical form of gramicidin was detected by circular dichroism spectroscopy and determined using 500 and 600 MHz NMR in $CaCl_2$/methanol solution. Measurements of TOCSY, DQF-COSY and NOESY spectra were converted into 604 distance and 48 torsional angle constraints for structure calculations. Stereospecific assignments and χ_1 angles were calculated using $^3J_{\alpha\beta}$, $d_{\alpha\beta}(i,j)$, $d_{N\beta}(i,j)$ and $d_{N\gamma}(i,j)$. χ_2 angles were determined using $d_{\alpha\delta}(i,j)$, $d_{N\delta}(i,j)$, $d_{\beta\delta}(i,j)$, $d_{N\gamma}(i,j)$ and $d_{\alpha\gamma}(i,j)$. The calculations of initial structures were performed using the distance geometry/simulated annealing method in XPLOR. The initial structures were further refined and energy minimized using simulated annealing/molecular dynamics methods. Back-calculations for every generated structure were also performed to check their consistency with the experimental data.

187 final structures with no violations above the threshold conditions (0.05 Å, 5°, 5°, 0.5 Å and 5° for bonds, angles, improper, NOE and cdihe, respectively) were produced from the 200 initial structures. Twenty structures with the lowest NOE energies were used for further analysis. The average r.m.s. deviations for the 20 structures are 0.64 Å for backbone and 1.1 Å for all non-hydrogen atoms.

Gramicidin in this form, with approximately 5.7 residues per turn, is a parallel double helical dimer. The length along the helix axis is about 30 Å and the inner pore diameter varies from 1 to 2 Å. It is different from all other gramicidin structures determined to date. The presence of Ca^{2+} stabilises a conformation that prevents the binding of monovalent cations. It is likely that this structure is related to a non-channel, antibiotic role of gramicidin.

© 1996 Academic Press Limited

Keywords: calcium binding; antibiotic structure; nuclear magnetic resonance; membrane polypeptide

Introduction

Gramicidin A is a linear polypeptide antibiotic synthesized by *Bacillus brevis* (Hotchkiss & Dubos, 1940). It contains 15 hydrophobic amino acids with an ethanolamine residue at the carboxyl terminus and a formyl group at the amino terminus. The sequence is (Sarges & Witkop, 1965):

formyl-L-Val-Gly-L-Ala-D-Leu-L-Ala-D-Val-L-Val-D-Val-L-Trp-D-Leu-L-Trp-D-Leu-L-Trp-D-Leu-L-Trp-ethanolamine

Abbreviations used: NMR, nuclear magnetic resonance; CD, circular dichroism; NOE, nuclear overhauser effect; COSY, correlated spectroscopy; TOCSY, total correlated spectroscopy.

The most characteristic feature of gramicidin is its sequence of alternating L- and D-amino acids. This molecule contains neither charged nor polar amino acids, so it is virtually insoluble in water but is soluble in a wide variety of phospholipids, alcohols and other organic solvents.

Being a relatively small and conformationally flexible polypeptide, gramicidin can adopt a number of different types of conformations, depending on its environment. The major types of gramicidin conformations have been classified into helical dimer or double helical structures (Urry, 1972; Veatch *et al.*, 1974). The helical dimer has two monomeric helices associated with each other N terminus-to-N terminus (Urry, 1972). This form has a helical pitch of 6.3 residues per turn and forms a

0022-2836/96/440757-13 $25.00/0

© 1996 Academic Press Limited

cylindrical tube with 12 parallel β-sheet-like intra-molecular hydrogen bonds between residues in adjacent turns of each monomer. The association between monomers in the helical dimer is via six inter-molecular hydrogen bonds. This form exhibits conductance specifically for monovalent cations. In synthetic saturated phospholipid membranes, it is the predominant conformation (Wallace *et al.*, 1981). Its conformation has been determined by 2D NMR in sodium dodecyl sulphate micelles (Arseniev *et al.*, 1985; Bystrov *et al.*, 1990) and from solid state NMR studies in orientated bilayers (Ketchem *et al.*, 1993). In contrast to the helical dimer form, gramicidin adopts a number of different conformations in organic solvents (Veatch *et al.*, 1974) and unsaturated lipids (Sychev *et al.*, 1993). In all these conformations, the two monomers are interwound and twisted into double-helical structures. The associations between the two monomers in the double helical motifs are as in a β-sheet with two monomer polypeptide chains running either parallel or antiparallel to each other and held together by hydrogen bonds. From thin layer chromatography and circular dichroism spectroscopy studies (Veatch *et al.*, 1974), four distinct species which could interconvert with each other were identified in organic solvents. These four structures were proposed to be: two different left-handed parallel double helices (species 1 and 2), which only differ in the stagger between their chains, a left-handed antiparallel double helix (species 3), and a right-handed parallel double helix (species 4). These conformers exhibit three distinct patterns in circular dichroism spectroscopy (Veatch *et al.*, 1974). A number of distinct sets of peaks were detected in a 2D NMR spectrum of the equilibrium mixture (Bystrov & Arseniev, 1988).

The first detailed structures of the double helical species were determined by X-ray crystallography as both the ion-free gramicidin from ethanol (Langs, 1988) and a CsCl complex from methanol (Wallace & Ravikumar, 1988). The crystal structures both have a left-handed antiparallel double helical motif, but the helical pitch is smaller and the diameter of pore is wider in the caesium-complexed form. A number of gramicidin structures have been determined by 2D NMR spectroscopy in different environments (Pascal & Cross, 1992, 1993; Zhang *et al.*, 1992; Ketchem *et al.*, 1993; Arseniev *et al.*, 1985). These studies revealed the detailed structures of a left-handed antiparallel double helix in ethanol/benzene solution (Pascal & Cross, 1993; Zhang *et al.*, 1992), and a right-handed parallel double helix in dioxane (Pascal & Cross, 1992) and provided a general view of the different species in equilibrium in ethanol (Bystrov & Arseniev, 1988). The structure of the left-handed antiparallel double helix solved in ethanol/benzene solution was found to be very similar to that of the ion-free form in the ethanol crystal. Although NMR studies to date have determined two types of high resolution gramicidin double-helical structures, left-handed antiparallel and right-handed parallel double helices, the high resolution structure of a parallel double-helical gramicidin has not yet been reported. Here, we describe a means of producing a homogeneous sample containing a left-handed parallel double-helical gramicidin in $CaCl_2$/methanol solution and its high resolution three-dimensional structure as determined by NMR spectroscopy.

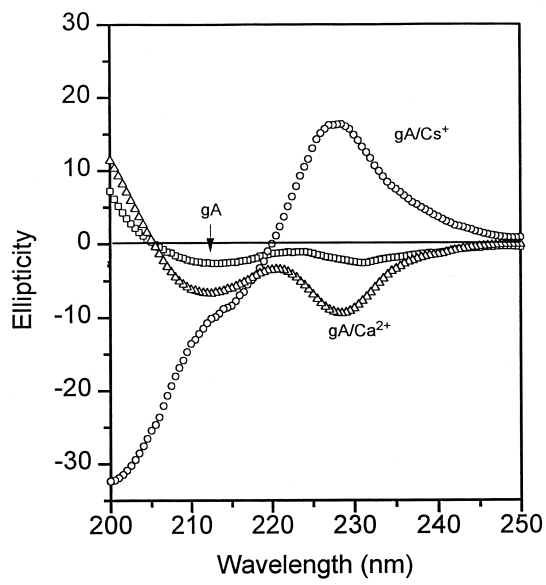

Figure 1. Circular dichroism spectra of ion-free gramicidin, Cs^+/gramicidin and Ca^{2+}/gramicidin. The concentrations of gramicidin, Cs^+, and Ca^{2+} are 0.8 mM, 16 mM and 4 mM, respectively.

Results

Circular dichroism spectra

Figure 1 shows the circular dichroism (CD) spectra of ion-free gramicidin, Cs^+-bound gramicidin and gramicidin in the $CaCl_2$/methanol solution. It can be seen that the CD spectrum of gramicidin in the $CaCl_2$/methanol solution is dramatically different from that of either the ion-free or the monovalent cation-bound forms.

NMR spectra

Figure 2(a) and (b) shows, respectively, the fingerprint region of a 50 ms NOESY spectrum with full sequential assignments, and a 60 ms TOCSY spectrum. The peaks in the spectra are well resolved. Besides the well defined peaks for gramicidin A, there are a few minor peaks which probably arise from gramicidin B and C (versions of the peptide with Phe or Tyr substituted for Trp at position 11, present in minor amounts in the naturally occurring samples), or other minor alternate structural forms of gramicidin A. In general, the NMR spectrum consists of a single set of resonances, showing that this dimeric form of gramicidin has a symmetric conformation.

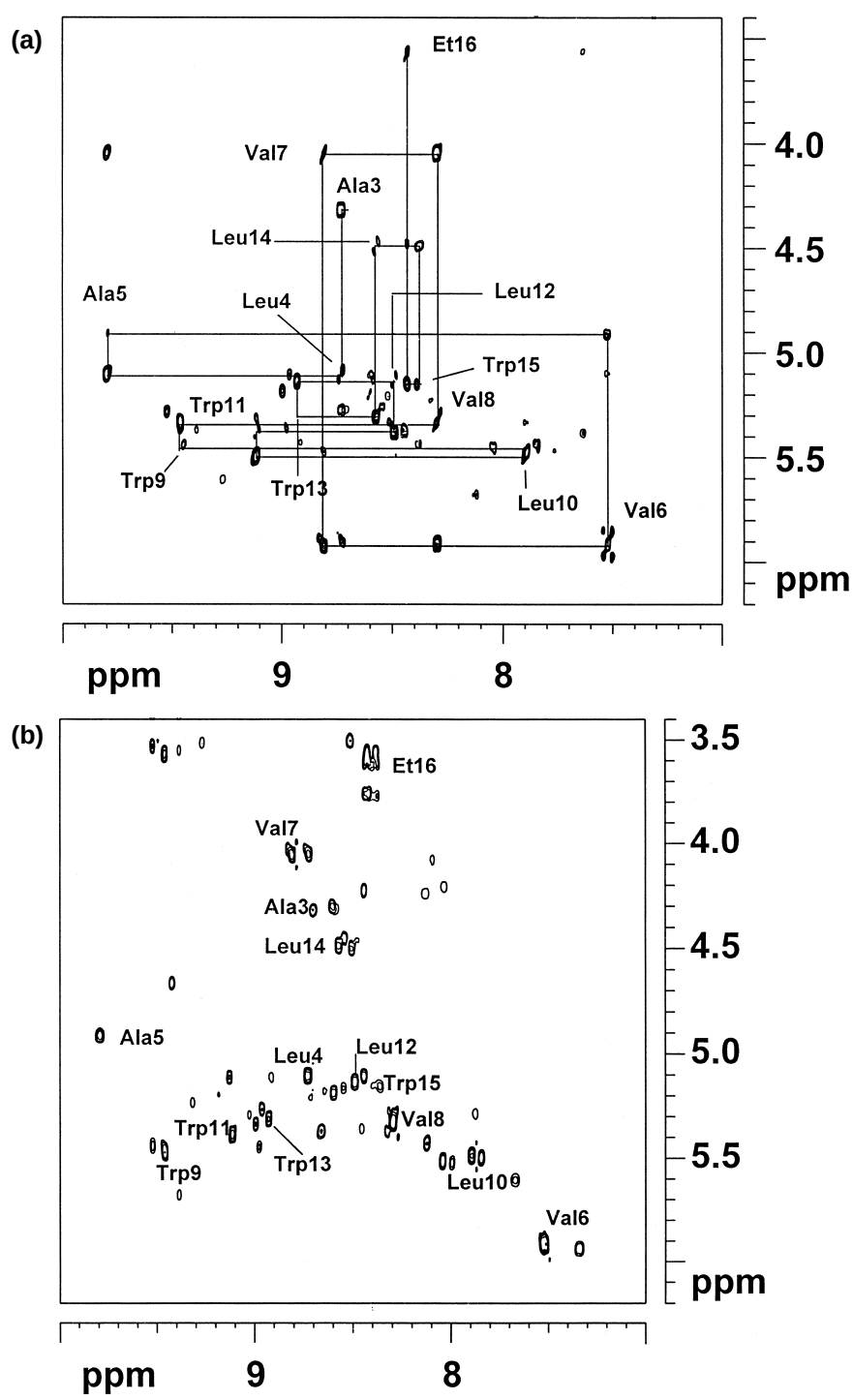

Figure 2. (a) The fingerprint (H^N-H^α) region of 50 ms NOESY and (b) 60 ms TOCSY 2D NMR spectra. In (a), the lines show the sequential walk assignments between each residue.

Resonance assignments

Spin system identifications and sequential resonance assignments were performed according to well-established procedures (Billeter *et al.*, 1982; Wuthrich, 1986). All spin systems can be identified except that of the formyl group at the N terminus. In Figure 2(a), it can be seen that strong $d_\alpha(i)$-$d_N(i+1)$ cross-peaks in the 50 ms NOESY spectrum can be unambiguously assigned for residues 3 to 16. The H^Ns assignments for Val1 and Gly2 were identified by changing the temperature (296 K). The chemical shifts of the H^α and other types of protons for these two residues were basically unaltered by temperature. Stereospecific assignments were determined by analysis of stereochemical relationships using $^3J_{\alpha\beta}$, $d_{N\gamma}(i,i)$, $d_{\alpha\beta}(i,i)$. Full assignment of the 250 ms NOESY system produced 280 intra-residue and inter-residue NOEs.

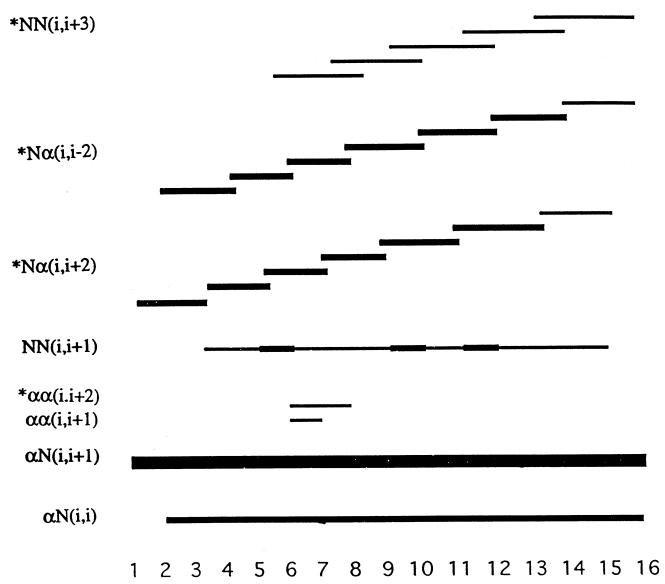

Figure 3. Summary of the NMR data used for the identification of secondary structural elements in Ca^{2+}-gramicidin. The thickness of the bars indicates the relative strength of the NOE cross-peaks. The symbol * indicates the inter-molecular NOE cross-peaks.

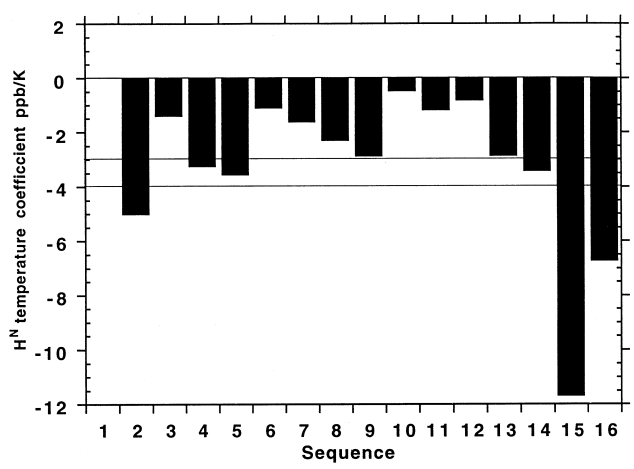

Figure 4. Plots of H^N chemical shift temperature coefficient *versus* sequence position.

Secondary structure

In the H^N-H^N region of the 250 ms NOESY spectrum, few weak $d_N(i)$-$d_N(i+1)$ and $d_N(i)$-$d_N(j)$ cross-peaks are observed. In the 250 ms NOESY spectrum for H^α-H^α region, only two NOE cross-peaks, i.e. H^α_8-H^α_9 and H^α_9-H^α_8 can be found. In combination with the observed strong $d_\alpha(i)$-$d_N(i+1)$ NOE, weak $d_N(i)$-$d_N(i+1)$ and lack of $d_\alpha(i)$-$d_\alpha(j)$ NOE peaks, this indicates that the secondary structure of gramicidin has the main features of a parallel β-sheet. The summary of the NMR data for the identification of secondary structure elements is shown in Figure 3.

Temperature dependence of NH chemical shifts

1D and 2D TOCSY ^{1}H NMR spectra were acquired over the temperature range from 275 to 325 K in 5 K increments. Chemical shifts were extracted and plotted *versus* temperature for the H^N resonances of residues 2 to 16. All data sets could be fitted to a linear function (with $R > 0.999$) except for Trp11 which appeared to show a biphasic temperature dependence. The temperature coefficients (ppb/K) extracted from the fitted data are shown in Figure 4.

Structure determination

The 280 NOE cross-peaks were converted into 104 distance constraints for the polypeptide backbone, and 456 distance constraints for the side-chains. All structure calculations were carried out in XPLOR. Initially only the 104 backbone constraints were used to generate a starting model to test whether the structure was a monomer or dimer. Possible monomeric structures were tested by assigning all distance constraints to intra-molecular interactions only, but the structures showed extra $d_\alpha(i)$-$d_\alpha(i+3)$ constraints which are not present in the NMR data. Hence, the possibility of a monomeric structure can be excluded.

The hydrogen bonds were assigned based on the results from the backbone motifs generated in the first stage and the temperature dependence of the NH chemical shifts. All hydrogen bonds assigned are of the inter-chain type. The arrangements of hydrogen bonds are generally similar to the proposed species 1 (Veatch *et al.*, 1974; Bystrov & Arseniev, 1988), being $H_N(i)$-$O(j+1)$ and $H_N(i)$-$O(j-3)$ where $j = i$ in residue number, i and j refer to the residues of different polypeptide chains of the dimer. It can be seen that the $H_N(i)$-$O(j+1)$ type occurs in all odd numbered residues from 3 to 13, and the $H_N(i)$-$O(j-3)$ type appears only for the even numbered residues from 6 to 14. The distances were set at 2.2 to 2.8 Å between the amide H and CO and at 2.7 to 3.3 Å between the amide N and CO (Baker & Hubbard, 1984; Mitchell & Price, 1990). No hydrogen bonds were assigned for Trp15, Trp16, Gly2 and Val1, since their temperature coefficients were higher than −0.4 ppb/K.

A final set of constraint conditions containing 604 distances, including 44 hydrogen bonds, 26φ and 18χ_1 and four χ_2 dihedral angle constraints were used to generate dimer structures. There are no long range ($i - j > 5$) distance constraints. The 26φ dihedral angles assigned do not include residues 1, 2 and 16 and were assigned as two angles, −120(±60)° and 120(±60)° for L-amino acids and D-amino acids, respectively. For χ_1 angles, only 60(±40)° and 180(±40)° were found for the 18 assigned χ_1 data. For the possible χ_2 angles, only those for Leu4 and Leu12 were found and were 60(±40)°. 187 structures which showed no violations above the threshold conditions (0.05 Å, 5°, 5°, 0.5 Å and 5° for bonds, angles, improper, NOE and

cdihe, respectively) were generated from 200 initial models after three cycles of simulated annealing raising the initial temperature from 1000 K to 3000 K with 6000 cooling steps. No rigid body, symmetry or shake functions were imposed on the structure calculations. The 20 structures with the lowest NOE energies (<27 kcal) were selected for further structure analysis. The statistical data are summarized in Table 1.

Structure analysis

The two chains in the dimer are designated as A and B respectively. Figure 5A and B summarises the distribution of NOE constraints and r.m.s. deviations for the backbone and side-chain heavy-atoms in the 20 "best" structures as a function of residue number. The total mean pairwise r.m.s deviations for the backbone heavy-atoms (N, C^{α}, C') and for all non-hydrogen heavy atoms are 0.64(±0.15) Å and 1.10(±0.20) Å, respectively. For the best defined region of the structures, i.e. residues 3 to 13, the mean pairwise r.m.s. deviations are 0.30(±0.12) Å for backbone heavy-atoms and 1.14(±0.21) Å for all non-hydrogen atoms, respectively. A comparison between the A and B chains of the lowest NOE energy structure shows no significant differences (r.m.s deviation <0.01 Å).

The r.m.s deviations for the 20 lowest NOE energy structures show that the conformations at the N terminus for either backbone (0.61 Å for Val1 and 0.31 Å for Gly2) or side-chains (1.38 Å for Val1 and 0.51 Å for Gly2) are more similar than those at the C terminus (for backbone, 1.46 Å for Eth16 and 0.6 Å for Trp15, and for side-chain, 2.35 Å for ethanolamine and 1.4 Å for Trp15). This is despite the fact that there are more NOEs for the C terminus (five for ethanolamine and 24 for Trp15) than for the N terminus (six for Val1 and five for Gly2). The reason could be that the structural constraints arising from Ala3 are more effective than those from Leu14. For the side-chains, the r.m.s. deviations for Leu4 (0.77 Å), Trp9 (0.73 Å), Trp13 (0.91 Å) and Trp15 (1.40 Å) are much higher than for the rest of the residues (average =0.41 Å). The r.m.s deviations for valine residues (~0.4 Å) are less than for leucine (~0.63 Å) and tryptophan (~0.88 Å) residues.

A Ramachandran plot was generated using PROCHECK-NMR (MacArthur *et al.*, 1994) for the family of 20 structures (Figure 6). The data points shown in the top and bottom right regions in the Ramachandran plot (normally a disallowed region) arise from D-amino acid residues. In general, all ϕ and ψ angles for all residues are within the acceptable regions in the Ramachandran plot and indicate that the whole molecule has a mainly β-strand structure. There are no distortions of bond length, bond angle, or the planarity of indole rings for any structures. The percentage of residues in favourable regions calculated is apparently poor, but this is due to the large number of D-amino

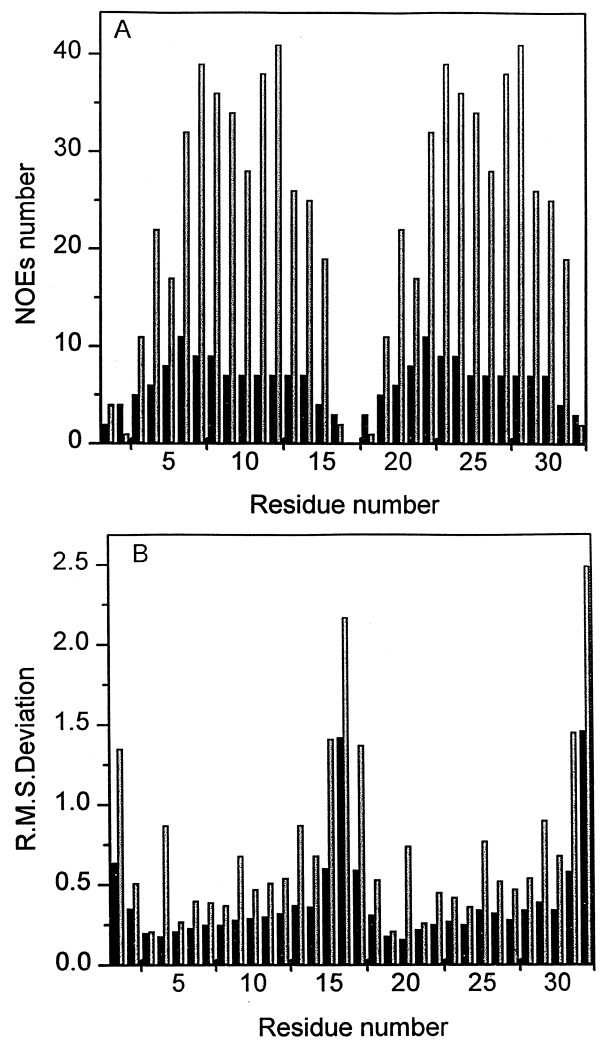

Figure 5. Plots as a function of residue number for (A) the number of backbone (dark bar) and side-chain (light bar) NOEs used in the final structure calculations and (B) r.m.s deviations within the family of 20 structures for the backbones (dark bar) and for the side-chains (light bar). The residue numbers 1 to 16 are for the A-chain and 17 to 32 are for the B-chain.

Table 1. Energetic parameters and r.m.s. deviations from experimental and structural constraints

	Ensemble structures	Lowest NOE energy structure
Energetic parameters (kcal mol^{-1})		
Total energy	84.55 ± 0.11	84.87
Bonds	5.47 ± 0.05	5.26
Angles	33.04 ± 0.07	36.74
Impropers	8.41 ± 0.11	10.43
van der Waals	16.25 ± 0.15	12.44
NOE restraints	25.60 ± 0.02	24.42
Dihedral restraints	0.23 ± 0.10	0.03
Deviations from experimental constraints		
r.m.s-NOE (Å)	0.024 ± 0.005	0.028
r.m.s-dih (deg)	0.22 ± 0.20	0.1
Deviations from ideal geometry		
r.m.s-bond (Å)	0.003 ± 0.001	0.003
r.m.s-angles (deg)	0.46 ± 0.04	0.44
r.m.s-impropers (deg)	0.41 ± 0.06	0.43

acids. If all D-amino acids are considered to be in favourable areas, then the equivalent resolution will improve to 3.0 to 3.5 Å. Analysis of ϕ and ψ angles for all residues of the family of 20 structures shows that the ϕ and ψ angles for all leucine residues, Val6 and 8, Trp13 and 15, and Ala3 residues are in the most favourable region, while Trp9, 11, Val7 and Ala5 residues show ϕ and ψ angles located in the additionally allowed area.

The orientations of the side-chains for Trp9, 11, 13 show lower variation than those of Trp15. This is because there are well defined χ_1 angles (180°) for Trp9, 11, 13 but not for Trp15. Although a large $^3J_{\alpha\beta}$ (>14 Hz) and a small $^3J_{\alpha\beta}$ (<5 Hz) are observed for all tryptophan residues, no H^N-H^β NOE peaks for Trp15 can be observed, so, its χ_1 angle cannot be uniquely determined. In addition, Figure 5A shows that there are large numbers of NOEs for the side-chains of Trp9 (34), Trp11 (38) and Trp13 (26), but only a few for Trp15 (19). Consequently, the r.m.s deviations are less than 0.7 Å for Trp9, 0.6 Å for Trp11 and 0.9 for Trp13, but greater than 1.4 Å for Trp15.

Description of the structures

Figure 7(a) shows a stereo view of the superimposed backbones of the family of 20 structures and Figure 7(b) shows the molecule (including all side-chains) for the structure with the lowest NOE energy. Its conformation is a left-handed parallel double helix with two monomers interwound. A hole is formed in the middle of the two interwound chains. All side-chains appear on the surface of the molecule. This arrangement results in all tryptophan residues in the C-terminal half of each molecule being located near the same end of the structure with their indole rings pointing toward the N terminus and the plane of the rings almost parallel to the helical axis. Other side-chains lie approximately perpendicular to the helical axis. The backbones exhibit a 2-fold symmetry about the helical axis, consistent with the observation of a single set of resonances in the NMR spectra.

The dimension of the central pore

Figure 8 displays the diameter of the central pore for the structure with the lowest NOE energy, calculated using the program HOLE (Smart *et al.*, 1993). The calculated length between the two pore ends is about 30 Å. The inside diameter along the central pore axis varies from 0.8 to 1.0 Å at the N terminus to about 2 Å at the end of the C terminus. The average diameter is about 1.2 Å. There is not enough room for cations or water to traverse the pore, but a rather open structure appears near the N-terminal end.

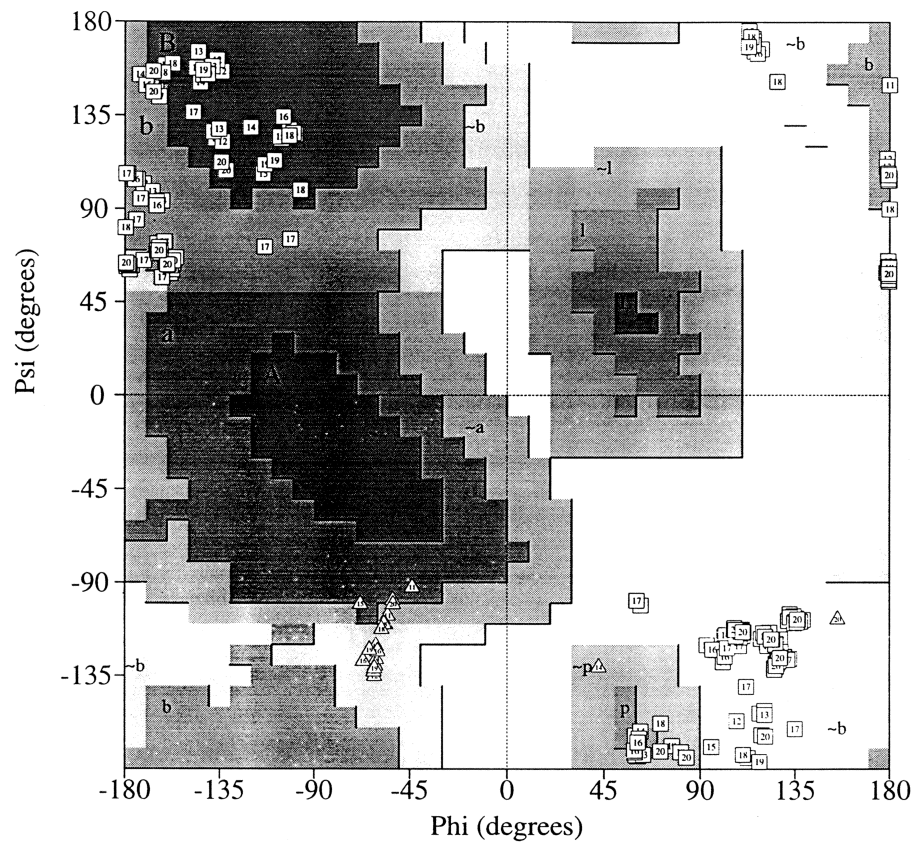

Figure 6. Ramachandran plot for the family of 20 lowest NOE energy structures of the left-handed parallel double-helical gramicidin. The numbers in the open squares represent the different models. In general, all angles are within allowed regions.

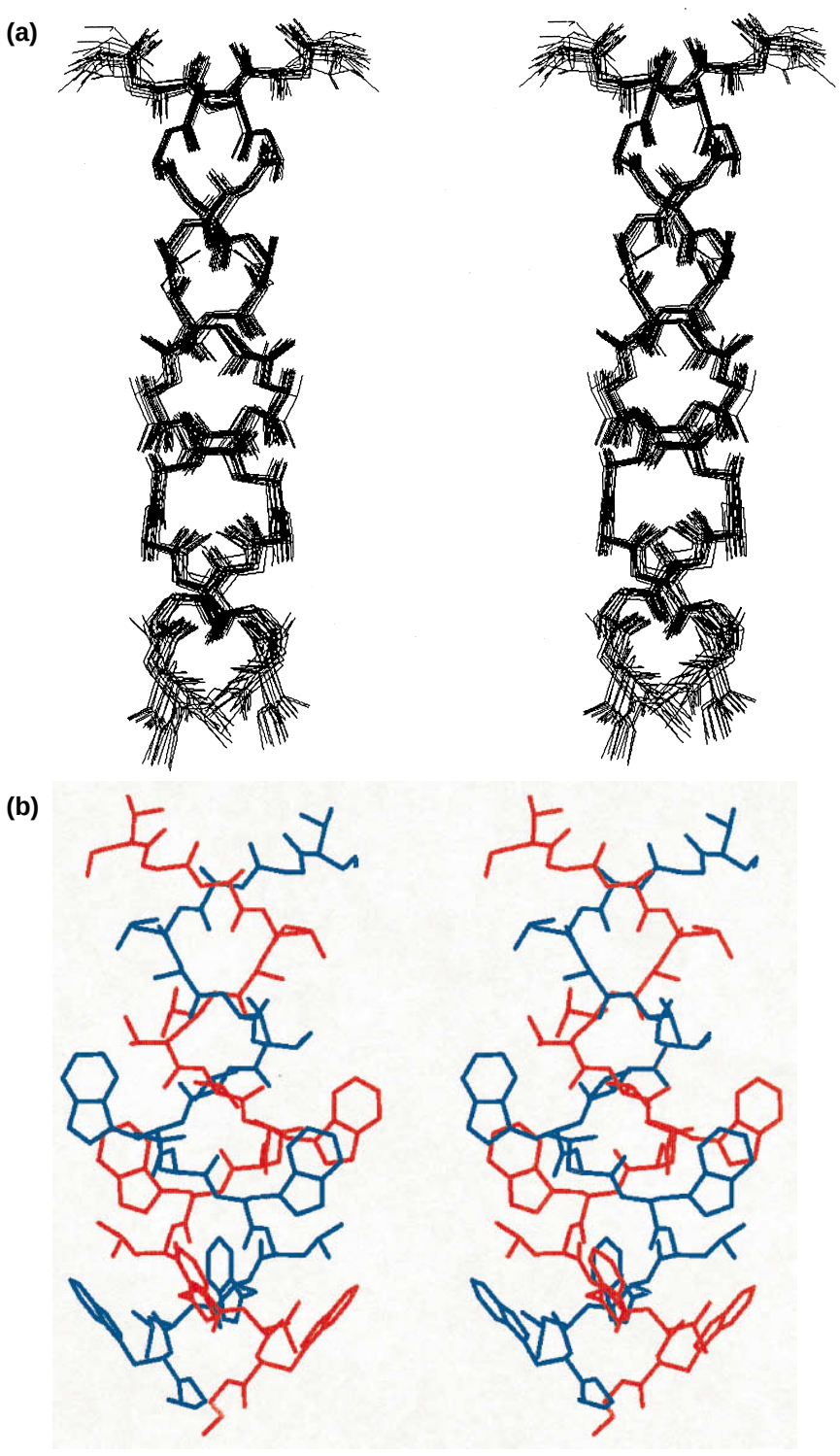

Figure 7. (a) Stereo view of the backbones of the family of 20 lowest NOE energy structures, (b) stereo view of the lowest NOE energy structure, indicating all its side-chains.

Surface electrostatic potential map

The calculations of the surface potential were performed on the 20 lowest NOE energy structures. The exterior dielectric constant was set to 32.7 D with an ion concentration of 0.1 M. The interior dielectric constant was varied from 2 to 80 in order to account for all possible situations, since there is no good available data for this value in a hydrophobic environment. Figure 9 shows the surface potential maps for the lowest NOE energy structure at an interior dielectric constant of 15 D. There is always a strong negative charge (red colour) around the N terminus with the different interior dielectric constants in all 20 models. Only a weak positive charge map appears at the C terminus when using high interior dielectric constants, but this disappears when low values of dielectric constants were used. The only negatively charged region was found to be located near the

Val1 residues. At an interior dielectric constant of 15 D, the total charge is −0.5 using the AMBER force field and −0.7 using the CHARMm force field.

Discussion

Comparison between the determined structure and proposed models

This left-handed parallel double helix is similar to model 1 proposed by Veatch *et al.* (1974) for the equilibrium mixture of conformations in ion-free methanol solvents. That model has the same helical pitch and same lack of stagger between monomers. The chemical shifts for individual residues in the NMR spectrum (in particular those for Gly2, Ala3, Val4 and Val8) are, however, not the same as those reported by Arseniev *et al.* (1985) in a preliminary study on the mixture of species, in which no structure was calculated, but consistency with the backbone models proposed by Veatch *et al.* (1974) was checked. For the remaining residues, the chemical shifts are, in general, in the same regions. The hydrogen-bonding patterns in the earlier work were assigned based only on the general solvent accessibilities but are identical to ours except near the N and C termini in which both the Arseniev and Veatch models show a less ordered structure, and therefore, their hydrogen-bonding pattern cannot be determined.

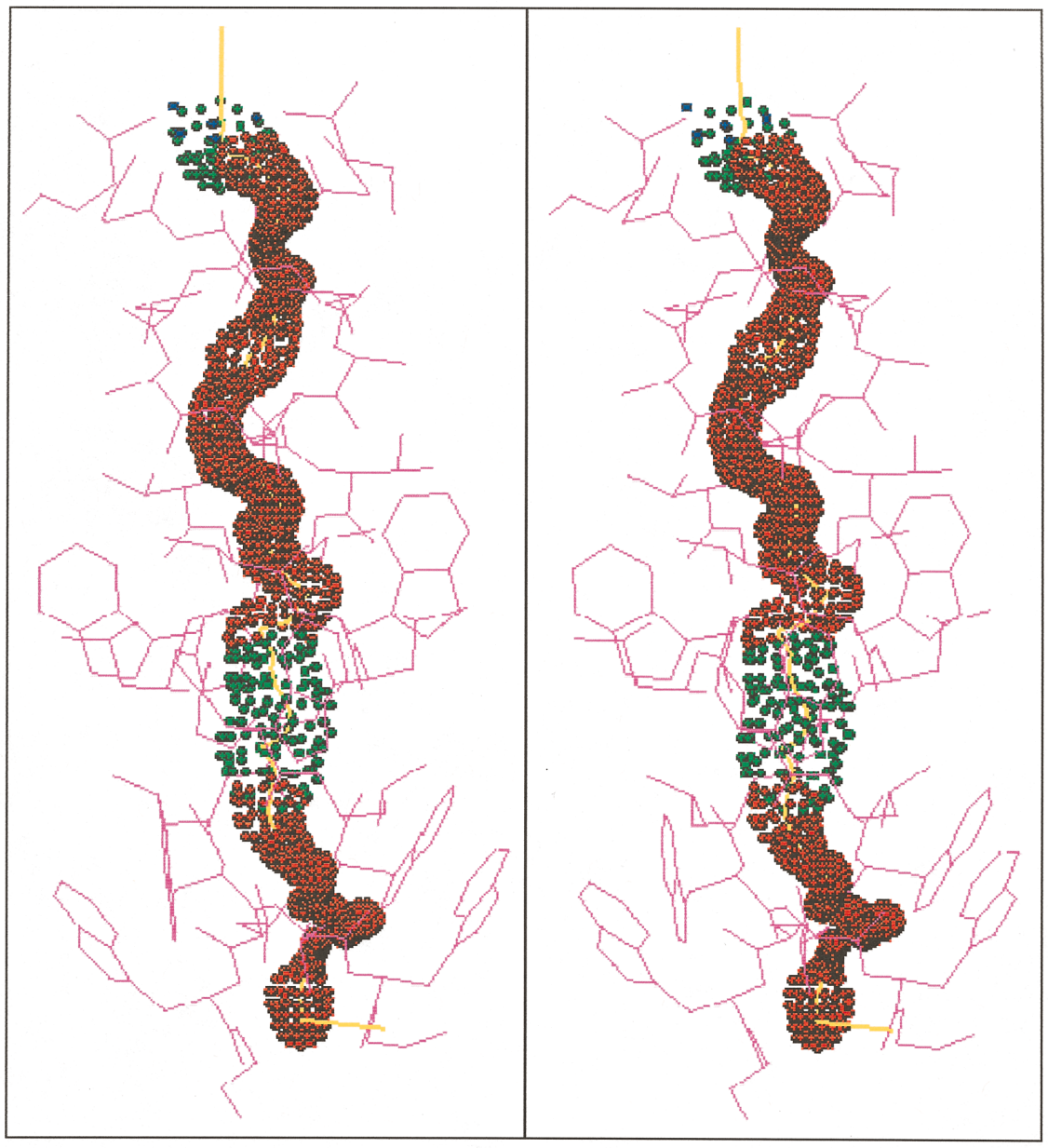

Figure 8. Diagram of the central hole dimensions of the lowest NOE energy structure calculated using the HOLE program. The dots show the outer surface of the largest sphere that can pass through the central hole. The green dots indicate the only regions large enough to accommodate water molecules.

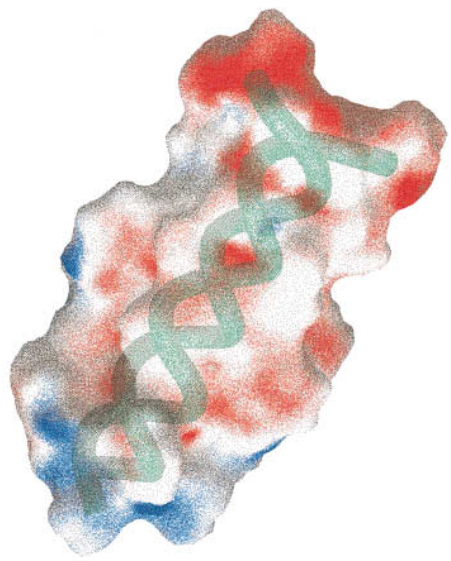

Figure 9. Plot of the surface potential map of the lowest NOE structure using GRASP. The dielectric constants were set at 32.7 D for the exterior and 15 D for the interior, respectively. The red colour represents the negative charge and the blue positive charge. The polypeptide backbones are represented by green "worms". It can be seen that a large negative charge is located at the N-terminal end.

Comparison was done of our NMR structure with the X-ray structure of the left-handed antiparallel double helix (Langs, 1988). Since the crystal structure has a different stagger between the two chains and the A and B chains run in opposite directions, a detailed comparison between these two conformations is not applicable, but the overall dimensions are roughly comparable. The r.m.s difference between each monomer chain running in the same direction is about 2.5 Å. The NMR structure is more symmetric but narrower in diameter than the crystal structure. The length of the NMR structure is slightly shorter (~30 Å) than the crystal structure. A general comparison between the various structures of gramicidin that have been determined is summarized in Table 2.

Hydrogen bonds

The temperature dependence of amide proton chemical shifts has previously been shown to be closely related to hydrogen bonding in peptides and proteins (Yee *et al.*, 1995). In polar, hydrogen-bonding solvents, such as methanol, amide protons which are accessible to the solvent show a larger temperature dependence of their chemical shifts (due to changes in the solute-solvent hydrogen bonding) than amide protons which are hydrogen-bonded to other parts of the peptide (and thus screened from the solvent). In particular, for beta sheet type structures, temperature coefficients of > −0.3 ppb/K are evidence for strong hydrogen-bonding, those < −0.4 ppb/K are evidence for solvent accessible, non hydrogen-bonded amides and intermediate values indicate weak hydrogen bonding. From Figure 4, it can be seen that for residues 6 to 13, the temperature coefficients are all > −0.3 ppb/K and are thus good evidence of strong hydrogen-bonding for the amide protons of these residues. Residues 4, 5 and 14 show intermediate values and are probably more weakly hydrogen-bonded.

Tryptophan residues

Tryptophan residues are very important in the functioning of gramicidin. They regulate not only the conductance and the interactions with lipids and with other molecules, but also the conformation. In different environments, the tryptophan residues adopt different orientations (Woolley *et al.*, 1992). Although it must be kept in mind that side-chain orientations in the crystal structures may be influenced by crystal packing, in methanol, the crystal structure shows that the tryptophan rings of gramicidin are more-or-less perpendicular to the helical axis (Langs *et al.*, 1991), while they are more parallel to the helical axis in ethanol crystals (Langs, 1988), in gramicidin-Cs^+ crystals from methanol and in lipids (Arseniev *et al.*, 1985; Pascal & Cross, 1992). The orientations of tryptophan side-chains in this NMR structure are more similar to those of the ethanol and Cs^+ complex, i.e. being parallel to the

Table 2. Summary of the structural dimensions of the different forms of gramicidin A

Environment	Method	Hand	Parallel/ antiparallel	Residue/ per turn	Length	Pore maxima
$CH_3CN(MeOH)/CDCl_3$[a]	NMR	r	A	7.2	27	4.0
$CH_3Cl(MeOH)$[b]	X-ray	l	A	6.4	26	4.9
EtOH[c]	X-ray	l	A	5.6	31	2.0
Dioxane[d]	NMR	r	P	5.7	27	2.6
EtOH/Benzene[e]	NMR	l	A	5.6	37	3.0
$CaCl_2(D_2OH)$[f]	NMR	l	P	5.7	30	2.0

[a] Arseniev *et al.* (1985); length determined from Val1(A)-N to Val1(B)-N.
[b] Wallace & Ravikumar (1988).
[c] Langs (1988).
[d] Pascal & Cross (1992); length determined from Val1-N to Eth-C1.
[e] Pascal & Cross (1995); length determined from formyl(A)-O to formyl(B)-O.
[f] This work; length determined from Val1-N to Eth-C1.

helix axis, but different from the ion-free structure in methanol.

It has been shown that tryptophan residues tend to intercalate their indole rings into water-lipid interfaces (Hu *et al.*, 1993; Koeppe *et al.*, 1994; Takeuchi *et al.*, 1990) on each side of the membrane. Since all tryptophan residues are located at one end of this parallel double-helical structure, it is expected that this conformation may be unfavourable in a membrane lipid environment.

Function of calcium cations

The function of $CaCl_2$ would appear to be to shift the equilibrium from the multiple interconvertible conformers present in methanol into a single stable conformation. What is the mechanism for this conversion? The results from the surface electrostatic potential calculations provide a clue. The gramicidin surface potential map shown in Figure 9 has a large negatively charged area around the N terminus in the region of Val1 and Gly2, primarily resulting from the helix dipole. This is found using different interior dielectric constants, different charge force fields and different generated structures. The calculated total charge is −0.7 using the CHARMm defined charge and −0.5 using the AMBER defined charge. This suggests that the open pocket at the N-terminal end may be the binding site for Ca^{2+}. This is consistent with the generated structures where the family of 20 lowest NOE energy structures shows a constrained conformation at the carbonyl group of Val1. This is an amazing result, since no NOE signals could be assigned for Val1 and the formyl group and is unusual because, normally, untethered termini in NMR structures have a wide array of conformations. The convergence at this position must be due to an extra feature holding the conformation, and the structure would indicate that Ca^{2+} play the key role. It is suggested that the four carbonyl groups from the Val1 residues and Gly2 form the possible binding site for Ca^{2+}. Although some weak positive charges appear around the areas of tryptophan indole rings and at the C-terminal end, they vary with the different interior dielectric constants used. Thus, it is expected that any possible binding of chloride anions, if at these sites, would be extremely weak.

Possible biological role of the parallel double helix

The role of the left-handed parallel double helix is very unlikely to be a conducting form due to its narrow central hole. Furthermore, being a parallel structure, it would form an asymmetric channel with respect to the two bilayer surfaces, which has not been observed for any conducting form of gramicidin. Then, what could be the biological role of this structure, if any? Although the functional studies of gramicidin have mainly examined its role in membrane permeability, its biological function as an antibiotic is seldom considered. It has been suggested that gramicidin can inhibit bacterial RNA synthesis by possibly binding to the σ unit of RNA polymerase (Bohg & Rietow, 1986; Paulus *et al.*, 1979). Paulus and co-workers showed that there was no relationship between the conductance of gramicidin and its inhibition of RNA synthesis. Many gramicidin analogues had no effect on membrane permeability but were still able to inhibit RNA polymerase. They noted that the eight amino acids at the N terminus had little influence on the inhibition of RNA polymerase, while the repeating D-Leu-L-Trp was essential for biological activity and may be the binding site. Our left-handed parallel double helix gramicidin has all its tryptophan residues at one end and in similar orientations relative to the backbone. Thus, it is possible, since this form is not a channel structure, that it could be a candidate for the form which binds RNA polymerase, although this is by no means proven.

Materials and Methods

Sample preparation

Gramicidin D was purchased from ICN Biochemicals. The purity of the material was checked by 1D proton NMR. *Methyl*-d_3-alcohol was purchased from Aldrich Chemicals (UK). Calcium chloride was purchased from Fisher Scientific (USA). All chemicals were reagent grade and used without further purification. For NMR experiments, the solution contained 20 mM gramicidin dissolved in *methyl*-d_3-alcohol with 0.1 M $CaCl_2$. In the circular dichroism spectroscopic measurements, a methanolic solution containing 8×10^{-4} M gramicidin was titrated with a stock solution of 0.5 M $CaCl_2$ in methanol.

Circular dichroism spectroscopy

Circular dichroism spectra were recorded using an AVIV 62DS spectropolarimeter with a wide-angle detector geometry. The optical rotation was calibrated using d-10 camphoursulphonic acid at wavelengths 192.5 and 290 nm. The wavelength was calibrated with benzene vapour. All measurements were made in Suprasil cells with pathlengths of 0.01 cm. In general, data were collected in the wavelength range from 200 to 250 nm using a 0.5 nm increment. For every CD spectrum reported, at least three individual samples and three repeated measurements of each sample were taken and averaged. The reported circular dichroism spectra were corrected for baseline using a solvent sample containing the same concentration of salt, and then smoothed using a Savitsky-Golay filter. All measurements were carried out at 25.0(±0.2)°C.

NMR spectroscopy

All NMR spectra were recorded at 303 K (except where indicated) at either 500 or 600 MHz on a JEOL GSX500 or Bruker AMX600. A ^1H sweep width of 14 ppm was used throughout. 1D spectra were collected using 32,768 points zero-filled to 65,536 and a relaxation delay of two seconds. 2D TOCSY and NOESY spectra were collected

using 4096 points in t_2 and 512 t_1 increments typically zero-filled to 8192 × 2048 points. A high digital resolution DQF-COSY spectrum was collected using 16,384 points in t_2 and 1024 t_1 increments for analysis of coupling constant data. Suppression of residual solvent signal (C^2H_3OH) was achieved using presaturation during the relaxation delay or by using the WATERGATE (Piotto *et al.*, 1992) sequence as indicated in the text.

2D data was typically processed with pre-multiplication of the time-domain data by a sine-bell squared function shifted by $\pi/2$. Analysis of crowded regions occasionally necessitated the shifting of this function by $\pi/3$ or $\pi/4$. Chemical shifts were referenced to the residual methanol resonance (3.3 ppm relative to 3-trimethylsilyl-(2,2,3,3-$^2H_4$)propionate).

Structure constraints

The NOE peaks were converted into three groups of distance ranges based on their integrated volume and build up in systems with different mixing times: strong peaks (1.8 to 2.5 Å), medium peaks (1.8 to 3.5 Å), and weak peaks (1.8 to 5.5 Å). All inter- or intra-molecular NOE peaks were distinguished later by back-calculation.

The calculations of the ϕ angles for the polypeptide backbone were achieved by analysis of $^3J_{NH\alpha}$ coupling constants using the Karplus equation (Karplus, 1959). The χ_1 angles for leucine 4, 12, 14, and tryptophan 9, 11, 13 were determined from the $^3J_{\alpha\beta}$ coupling constants, $d_{\alpha N}(i,i)$ and $d_{NN}(i,i)$ data and consideration of the stereochemistry of H^N, C^α, and C^β protons, assigned as one of three rotamers of 180°, 60° and −60°. Values of χ_2 for leucine 4 and 12 were also able to be calculated by the careful comparison of the stereochemistry of N_{H_2}, C^α, C^β and C^γ protons and using $d_{\alpha\beta}(i,i)$, $d_{NN}(i,i)$, $d_{\beta\gamma}(i,i)$, $d_{N\gamma}(i,i)$ and $d_{\alpha\gamma}(i,i)$ data.

Structure calculations

Structure calculations were performed in XPLOR, version 3.1, using the modified full-hydrogen topology and force field files (Brünger, 1992). The calculation included covalent geometry, planarity and repulsive van der Waals terms. The formyl group was created as a preresidue in the topology file and attached directly to Val1 during the creation of template coordinates. The ethanolamine group was defined as a new residue in the topology file. The conversion of L-amino acids into D-amino acids was accomplished at the stage of creating the template coordinate file using the LTOD patch function. For methyl groups, a pseudoatoms function which calibrated its specific bonds from the reference coordinate set (provided by program) was applied to the calculation. A restraining function of the distance between the geometric centres was used to calculate the NOE constraints energy.

Structure calculation proceeded in two stages: In the first stage, structure calculation started with no model, and only backbone distance constraints obtained from NOE cross-peaks were used to generate structures for all possible monomeric and dimeric models and to resolve any ambiguity in backbone NOE assignments. The second stage involved a full structure calculation using resolved backbone and other NOE distance and dihedral angle constraints.

Initial structures were calculated using the random/simulated annealing protocol (Nilges *et al.*, 1988). All backbone NOE constraints were assigned as both inter- and intra-molecular distances. The protocol used a soft-square function to calculate NOE constraint energies and commenced with simulated annealing by gradual cooling from 1000 K in time steps of 0.4 ps. Then, 3 fs of restrained molecular dynamics was performed with the initial van der Waals weighting at a low value (0.002). The created structures were further examined by back-calculation and compared to experimental data to properly assign the backbone inter- and intra-molecular distance constraints for subsequent structure calculations.

In the second stage, a full set of NOE and dihedral angle constraints was used to calculate structures in XPLOR, using distance geometry/simulated annealing methods. This protocol contains several steps, generating embedded sub-structures, embedding and metrising sub-structures and regularising the metrised full-structures. Only energy minimization was performed using the Powell function in the first two steps to generate structures. The regularisation of the full-structures was achieved by five cycles of molecular dynamics of 5 fs throughout and followed by simulated annealing which slowly cooled the initial temperature of 2000 K to 100 K in 50 K decrements. The repulsive van der Waals energy term was given the initial weight of 20 and reduced to 0.003 in the final step of the energy minimisation loop. These structures were then refined by simulated annealing using the same conditions as in the regularisation and followed by energy minimisation using the Powell function. The resulting structures were subjected to NOE back-calculation (see below) for several cycles in order to re-define ambiguous inter- *versus* intra-strand NOE constraints. The refined constraints data were then used to re-generate a set of structures which were again refined by three cycles of simulated annealing and energy minimisation to generate final structures. The initial temperature was raised from 1000 K for the first cycle to 3000 K for the final cycle, slowly cooling to 300 K throughout in 50 K decrements, including 3 fs of restrained energy minization in the final cycle of refinement. The acceptable final structures all had violations below 0.05 Å, 5°, 5°, 0.5 Å and 5° for bonds, angles, improper, NOE and dihedral angle restraints, respectively. There were no large amplitude dynamics which gave rise to any larger violations.

The back-calculation method considered only internal motions for the relaxation matrix (Keepers & James, 1984). The "model-free" approach (Lipari & Szabo, 1982) was used as the spectral density term which contains two parameters, correlation time for the measure of the internal motion and an order parameter for the measure of the spatial restriction of the motion. The calculation was based on the structure with the lowest NOE energy from the particular cycle of structure calculations. Conditions were set as 0.75 ps for the correlation time and three categories of the order parameter, 0.85 for H^N-H^α, 0.8 for H^α or H^N to other protons and 0.65 for others, as recommended by Brünger (1992). Only the 250 ms mixing time NOESY system was calculated and used for reference.

Structure analysis

The quality of generated structures was tested using the PROCHECK-NMR program (MacArthur *et al.*, 1994). The calculation of r.m.s. deviations between grouped structures was achieved using XPLOR. The surface electrostatic potential was calculated using the program GRASP (Nicholls *et al.*, 1993) with the dielectric constant

set at 32.7 D for the exterior and varied from 2 D to 80 D for the interior and the concentration of salt set to 0.1 M. The pore dimension calculation was performed on the lowest NOE energy structure using the program HOLE (Smart *et al.*, 1993) in which a hard core model was used to account for the atom radii. The coordinates have been deposited in the Brookhaven Protein Data Bank (accession code 1MIC).

Acknowledgements

This work was partially supported by a project grant (to B.A.W.) and Biomolecular Science Centre grant from the B.B.S.R.C. We also thank the ULIRS 500 MHz Biomedical NMR Centre at Birkbeck College and the ULIRS 600 MHz NMR Centre at Queen Mary and Westfield College for NMR facilities.

References

Arseniev, A. S., Barsukov, I. L., Bystrov, V. F., Lomize, A. L. & Ovchinnikov, Yu. A. (1985). ^{1}H-NMR study of gramicidin-A transmembrane ion channel. *FEBS Letters*, 186, 168–174.

Baker, E. N. & Hubbard, R. E. (1984). Hydrogen-bonding in globular proteins. *Prog. Biophys & Mol. Biol.* 44, 97–179.

Billeter, M., Braun, W. & Wuthrich, K. (1982). Sequential resonance assignments in protein ^{1}H-nuclear magnetic resonance spectra. Computation of sterically allowed proton-proton distances and statistical analysis of proton-proton distances in single crystal protein conformations. *J. Mol. Biol.* 155, 321–346.

Bohg, A. & Ristow, H. (1986). DNA-supercoiling is affected *in vitro* by the peptide antibiotics tyrocidine and gramicidin. *European J. Biochem.* 160, 587–591.

Brünger, A. T. (1992). *X-PLOR version 3.1. A System for X-ray Crystallography and NMR.* Yale University, New Haven, CT.

Bystrov, V. F. & Arseniev, A. S. (1988). Diversity of the gramicidin A spatial structure. Two-dimensional ^{1}H NMR study in solution. *Tetrahedron*, 44, 925–940.

Bystrov, V. F., Arseniev, A. S., Barsukov, V. I., Golovanov, A. P. & Maslennikikov, I. V. (1990). The structure of the transmembrane channel of gramicidin A: NMR study of its conformational stability and interaction with divalent cations. *Gazz. Chim. Ital.* 120, 485–491.

Hotchkiss, R. D. & Dubos, R. J. (1940). Fractionation of bactericidal agent from cultures of a soil bacillus. *J. Biol. Chem.* 132, 791–792.

Hu, W., Lee, K. C. & Cross, T. A. (1993). Tryptophans in membrane proteins: Indole ring orientations and functional implications in the gramicidin channel. *Biochemistry*, 32, 7035–7047.

Karplus, M. (1959). Contact electron-spin interaction of nuclear magnetic moment. *J. Phys. Chem.* 30, 11–15.

Keepers, J. W. & James, T. L. (1984). A theoretical study of distance determinations from NMR 2 dimensional nuclear overhauser effect spectra. *J. Magn. Reson.* 57, 404–426.

Ketchem, R. R., Hu, W. & Cross, T. A. (1993). High resolution conformation of gramicidin A in a lipid bilayer by solid state NMR. *Science*, 261, 1457–1460.

Koeppe, R. E., II, Killian, J. A. & Greathouse, D. V. (1994). Orientation of the tryptophan 9 and 11 side chains of the gramicidin channel based on deuterium nuclear magnetic resonance spectroscopy. *Biophys. J.* 66, 14–24.

Langs, D. A. (1988). Three-dimensional structure at 0.86 A of the uncomplexed form of the transmembrane ion channel peptide gramicidin A. *Science*, 241, 188–191.

Langs, D. A., Smith, G. D., Courseille, C., Precigoux, G. & Hospital, M. (1991). Monoclinic uncomplexed double-stranded, antiparallel, left-handed β-5.6-helix (1↓β-5.6) structure of gramicidin-A. Alternate patterns of helical association and deformation. *Proc. Natl Acad. Sci. USA*, 88, 5345–5349.

Lipari, G. & Szabo, A. (1982). Model-free approach to the interpretation of nuclear magnetic resonance relaxation in macromolecules. 1. Theory and range of validity. *J. Am. Chem. Soc.* 104, 4546–4559.

MacArthur, M. W., Laskowski, R. A. & Thornton, J. M. (1994). Knowledge-based validation of protein structure coordinates derived by X-ray crystallography and NMR spectroscopy. *Curr. Opin. Struct. Biol.* 4, 731–737.

Mitchell, J. B. O. & Price, S. L. (1990). The nature of the N-H O=C hydrogen-bond. An intermolecular perturbation theory study of the formamide formaldehyde complex. *J. Comput. Chem.* 11, 1217–1233.

Nilges, M., Clore, G. M. & Gronenborn, A. M. (1988). Determination of 3-dimensional structures of proteins from interproton distance data by dynamical simulated annealing from a random array of atoms. Circumventing problems associated with folding. *FEBS Letters*, 239, 129–136.

Nicholls, A., Bharadwaj, R. & Honig, B. (1993). GRASP-graphical representation and analysis of surface properties. *Biophys. J.* 64, A166.

Pascal, S. M. & Cross, T. A. (1992). Structure of an isolated gramicidin A double helical species by high resolution nuclear magnetic resonance. *J. Mol. Biol.* 226, 1101–1109.

Pascal, S. M. & Cross, T. A. (1993). High resolution structure and dynamic implications for a double-helical gramicidin A conformer. *J. Biomol. NMR*, 3, 495–513.

Paulus, H., Sarkar, N., Mukherjee, P. K., Langley, D., Ivanov, V. T., Shepel, E. N. & Veatch W. (1979). Comparison of the effect of linear gramicidin analogues on bacterial sporulation, membrane permeability, and ribonucleic acid polymerase. *Biochemistry*, 18, 4532–4536.

Piotto, M., Saudek, V. & Skeenár, V. (1992). Gradient-tailored excitation for single quantum NMR spectroscopy of aqueous-solutions. *J. Biomol. NMR*, 2, 661–665.

Sarges, R. & Witkop, B. (1965). Gramicidin A. V. The structure of valine- and isoleucine-gramicidin A. *J. Am. Chem. Soc.* 87, 2011–2020.

Smart, O. S., Goodfellow, J. M. & Wallace, B. A. (1993). The pore dimensions of gramicidin A. *Biophys. J.* 65, 2455–2460.

Sychev, S. V., Barsukov, L. I. & Ivanov, V. T. (1983). The double π-π-5.6 helix of gramicidin A predominates in unsaturated lipid membranes. *Eur. Biophys. J.* 22, 279–298.

Takeuchi, H., Nemoto, Y. & Harada, I. (1990). Environments and conformations of tryptophans side chains of gramicidin A in phospholipid bilayers studied by Raman spectroscopy. *Biochemistry*, 29, 1572–1579.

Urry, D. W. (1972). The gramicidin A transmembrane channel: a proposed π(L,D) helix. *Proc. Natl Acad. Sci. USA*, 69, 672–676.

Veatch, W. R., Fossel, E. T. & Blout, E. R. (1974). The conformation of gramicidin A. *Biochemistry*, *13*, 5249–5256.

Wallace, B. A. & Ravikumar, K. (1988). The gramicidin pore: crystal structure of a cesium complex. *Science*, *241*, 182–187.

Wallace, B. A., Veatch, W. R. & Blout, E. R. (1981). Conformation of gramicidin A in phospholipid vesicles: circular dichroism studies of effects of ion binding, chemical modification, and lipid structure. *Biochemistry*, *20*, 5754–5760.

Woolley, G. A., Durm, A. & Wallace, B. A. (1992). Gramicidin-lipid interactions induce specific tryptophan side chain conformations. *Biochem. Soc. Trans.* *20*, 864–867.

Wuthrich, K. (1986). *NMR of Proteins and Nucleic Acids*, John Wiley and Sons, New York.

Yee, A. A., Babiuk, R. & O'Neil, J. D. J. (1995). The conformation of an alamethicin in methanol by multinuclear NMR spectroscopy and distance geometry/simulated annealing. *Biopolymers*, *36*, 781–792.

Zhang, Z. L., Pascal, S. M. & Cross, T. A. (1992). A conformational rearrangement in gramicidin A. From a double-stranded left-handed to a single-stranded right-handed helix. *Biochemistry*, *31*, 8822–8828.

Edited by P. E. Wright

(Received 22 May 1996; received in revised form 12 September 1996; accepted 21 September 1996)

Supplementary material comprising one Table, is available from JMB On-line.